Journal of Materials Chemistry A

Accepted Manuscript

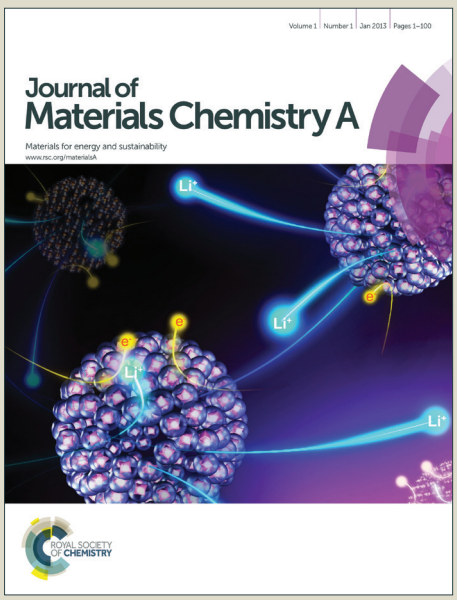

ROYAL SOCIETY OF CHEMISTRY

www.rsc.org/materialsA

Journal of Materials Chemistry A

RSCPublishing

ARTICLE

Bioinspired Design of a Photoresponsive Superhydrophobic/oleophilic surface with Underwater Superoleophobic Efficacy

I. E. Palamà,[a] S. D'Amone, [a] M. Biasiucci,[b,c] G. Gigli[a,d,e] and B.Cortese[a,b]

Cite this: DOI: 10.1039/x0xx00000x

Received 00th January 2012,
Accepted 00th January 2012

DOI: 10.1039/x0xx00000x

www.rsc.org/

Oil spills at sea are a severe global environmental issue. Smart materials with controllable wettability are of global challenging interest in oil/water related applications. Nature offers a versatile platform of remarkable hierarchical structures with a chemical component, which provides bioinspired solutions for solving many challenges. In this study, an approach to achieve robust superhydrophobic/oleophobic on flexible polydimethylsiloxane (PDMS) surfaces which mimics the hierarchical morphology of the natural lotus leaf surface is showed. The structure is prepared by hydrothermal assembly of zinc oxide nanorods onto the microstructured surface, which resulted in an underwater superoleophobic surface with oil contact angle up to 153° which can effectively prevent the surface from being polluted by oils. Our results are significant in terms of their importance to academic research and industrial applications and may lead to an innovative impact in the science field.

1 Introduction

Mother Nature's masterpiece the so called "*Lotus Effect*" and several other examples of natural superhydrophobic surfaces such as butterfly wings,[1] duck feathers,[2] legs of the water strider,[3] the desert beetle,[4] and fish scales[5] have long been an important topic for materials science, buoyed by the overwhelming role in both fundamental research and technological applications.[6-8] Learning from nature provides indispensable source of inspiration to develop new techniques and methodologies to construct artificial advanced functional materials. The common key to superhydrophobic surfaces lies, in fact, in the combination of the surface chemical compositions and the topographic structures which help to realize the decontamination, drag reduction, or even water collection.[6,9] Spurred by the challenge to understand the complementary roles of the two wetting key parameters, surface energy and roughness, an ever-increasing number of heterostructured surfaces, mimicking the lotus leaf structural morphology have been developed to fabricate such special super-antiwetting surface.[10-12] Of late, new research focus has also been aimed on surfaces that may repel liquids other than water, both in air and in aqueous media because of the frequent occurrence of oil spill accidents due to the offshore oil production and transportation.[13] The wettability of oil on a material surface, when submerged in an aqueous environment, has a critical role in many practical applications, such as water/oil separation, self-cleaning and oil-repellent coatings.[14-18] Moreover a surface with controlled oil wettability, or more desirably a smart surface that switches its oil wettability in response to external stimuli in aqueous media, would offer great promise in the design and fabrication of intelligent materials for advanced applications.[19] However, research on underwater interface characteristics remains a challenge, as most of the substrates that are oleophobic in air typically loses its oleophobicity under water, and vice versa.[20-22] What is more, an understanding of the oleophobic wetting behaviour with respect to the multi-scale microstructure and chemical properties is still missing.[23] Most of the reported existing methods to prepare superoleophobic surfaces in aqueous media emphasize the use of hydrophilic chemistry in combination with hierarchical surface structures introducing specially designed patterns, such as overhang structures and re-entrant surface curvatures or by modifying the surface chemistry with a coating of extreme low surface energy materials such as fluorochemicals and fluoropolymers resulting in considerable decrease in surface

energy.[24-33] Still, achieving optimal surface designs for such behaviour requires lithographic processes, and various isotropic and anisotropic etchings that are too complex for industrial applications. Specific functionalization of an artificially roughened surface with dynamic tunable wettability have become a core of much more high scientific and economic interest.[34-36] Micro/nano patterned surfaces with dissimilar wetting properties have been achieved using hierarchical structured mesh coated with aligned ZnO nanorod arrays.[37-38] However flexibility of the substrates becomes a more interesting topic. Although the mesh can be used for oil water separation, it is still a challenge for a metal interconnect to work under ultra-large strains and underwater. What is more crevice corrosion is a serious problem, both economically and operationally, for engineering systems such as aircraft, automobiles, and underwater applications such as pipelines, and naval vessels. On the other hand, the high flexibility of the PDMS facilitates deformation into any shape and can be compressed repeatedly in air or liquids without collapsing. Moreover PDMS is a low-cost efficient material with considerable absorption capacity, stable performance, and prospect to yield to a large-scale template. Due to the broad range of potential applications of underwater superoleophobic surfaces, there is therefore a need for a deeper understanding of not only how to fabricate such surfaces using simple methods, but also how specific surface properties, such as morphology, roughness, and surface chemistry, affect surface wetting and stability.

Dynamic photo-tunable with different wetting states, i.e., contact mode, between UV illumination and storage in the dark have been reported using various transition-metal oxides, such as ZnO.[37-38] ZnO nanostructures exhibit in fact reversible wettability by altering external stimuli such as UV light illumination. Here, inspired by the lotus leaf structure, we applied a simple and practical hydrothermal approach to fabricate large scale ZnO nanorods on microstructured PDMS substrates under ambient conditions.[20] The as-prepared environment-responsive surface exhibits superhydrophobic property in air, and changes to excellent superoleophobicity underwater. Most interestingly in combination with fluorosilane treatment, we were able to reverse the oleophilic capacities of the surface obtaining oleophobic substrates both in air and underwater. Because of the deformable flexible structure of the PDMS, and with the superwetting/antiwetting properties of the ZnO nanorods these substrates would be a versatile platform in a wide range of applications and can be considered to be promising candidates for designing novel water-removing materials for oil/water separation. The presented concept can significantly enlarge and open up area of functional interfacial materials with special wettability and new fields of applications for low-cost flexible solution based oil/water applications.

It is worth noting also that the control of wettability by both water and oil on one surface (hydrophilicity/hydrophobicity and oleophilicity/oleophobicity) reported so far have been focused on the wettability by either water or oil and barely been studied underwater, and the nanorod morphology of ZnO is rarely reported in oleophobic applications.[34-38]

2 Experimental section

Materials and microfabrication

Fig. 1 shows the fabrication procedures for the production of a flexible superhydrophobic structure consisting of ZnO nanowires and PDMS.

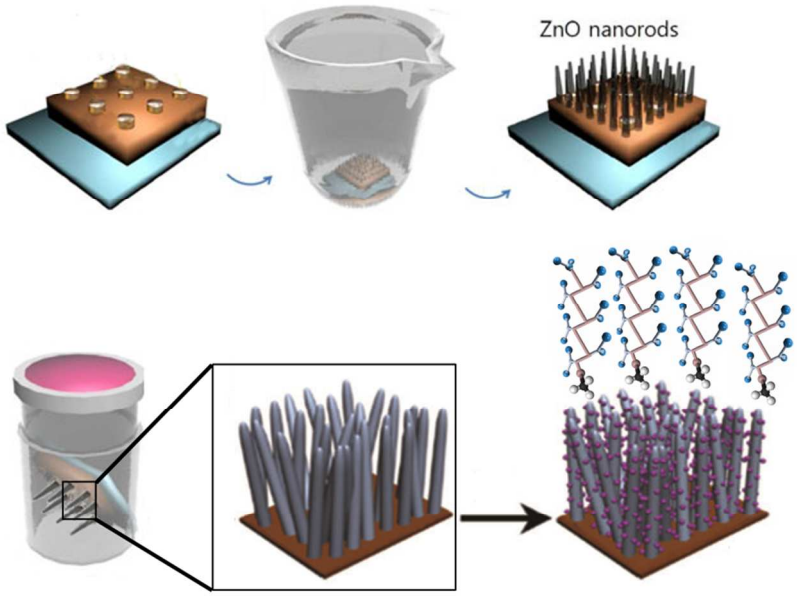

Fig. 1 Schematic description of the preparation of superhydrophobic PDMS-coated ZnO nanorod arrays onto the PDMS micropillars and subsequent modification with TFTS.

Microstructure fabrication: Negative relief SU-8 (Microchem) masters were fabricated following protocols from the manufacturer. SU-8 2010 was spin-coated onto cleaned silicon wafers to a thickness of ~20 μm, and patterned by conventional photolithography to yield an array of micropits ranging in diameter and center to center pitch from 10 to 70 μm. Regions of the master were intentionally designed without microgrooves to serve as flat surfaces for control experiments. The resulting structures were silanized by exposure to (tridecafluoro-1,1,2,2-tetrahydrooctyl)-1-trichlorosilane while under vacuum for 30 minutes. Polydimethylsiloxane (PDMS; Sylgard 184, Dow Corning, MI) base and curing agents were thoroughly mixed in a 10 : 1 ratio (w/w), degassed under vacuum, cast against the SU-8 master and cured at 60 °C for at least 4 hours. The positive replica PDMS slab was then carefully peeled from the master.

Fabrication of ZnO seed layer: The synthesis process involved two main steps as reported in the literature.[12] Details are described as follows: First, a five mM solution of inorganic precursor zinc acetate dehydrate (99.999%, Aldrich) in ethanol was made under vigorous stirring at 60 °C for 1 h. This solution (70 μL) was spread over the entire substrate and was allowed to evaporate for 25 s before rinsing with a copious amount of ethanol for each time to form a uniform ZnO seed layer. Between coatings the substrates were annealed at 120 °C for 15 min to ensure particle adhesion onto the substrate surface. The zinc acetate coating procedure was repeated four additional times.

Fabrication of ZnO Nanorods: Growth of nanorods was carried out suspending the substrates in an aqueous solution of zinc nitrate hexahydrate (50–75m M), HMTA (25 m M) at 100 °C for a pre-determined time from 0.5 h to 5h, depending on the desired length of nanorods. Finally the samples were thoroughly rinsed using deionized water to remove any residual salt or amino complex and allowed to dry in air at room temperature. All experiments described in hereafter were carried out under the typical conditions mentioned above.

Surface coating deposition: The self-assembled coatings were formed using a vapour deposition process. The samples were placed in a desiccator together with a small petri dish containing ≈1 mL of the (tridecafluoro-l,1,2,2-tetrahydrooctyl)-1trichlorosilane liquid. The desiccator was pumped down to ≈10 kPa. The pump was then shut off and the valve was closed so that the silane liquid could evaporate in the low-pressure environment of the desiccator and attach to the surfaces.

Characterization

Contact Angles measurements: The hydrophobicity of the lotus-leaf-like different systems was measured by means of the water contact angle (CA) using an OCA 20 contact angle system (Data Physics Instrument GmbH, Germany) at ambient temperature. To measure the contact angles of oil drops in aqueous media, we used two oils, diiodoemthane (Aldrich, density =3.325, surface energy (γ_{sv}) = 50.8 mN/m (γ_d= 48.5, γ_p = 2.3)) and olive oil (density = 0.930 g/ml, (γ_{sv}) = 32.6 mN/m (γ_d= 31.2, γ_p = 1.4)). A transparent glass chamber with the attached sample to the bottom was fabricated, and deionized water poured in. After 1 h of rest, a drop of oil (~3-6 μL) was placed on the substrate, and the contact angle of the drop was measured at room temperature. An average contact angle value was obtained by measuring at three different positions of the same pattern. The roll-off angles were measured by placing a specimen on a level platform and inclining the stage. Water and oil droplets (50, 100, and 500 μL) were placed onto the surface, and the angle of the stage was recorded when the drops began to roll off. The image of liquid droplets on the surface has been obtained using the digital camera of the OCA 20 contact angle system.In the ultraviolet (UV) irradiation tests, four 15 W low-pressure mercury lamps (λ = 265 nm) were used as the UV irradiation source; the distance between the UV light source and the sample was approximately 12 cm. After the UV irradiation, the films were placed in the dark for 7 days, new superhydrophobic measurements of the surfaces was obtained again for each sample.

Surface characterization: Low-resolution SEM characterization of the substrates was performed with a RAITH 150 EBL instrument. Typically, the images were acquired at low accelerating voltages (less than 5 kV) using short exposure times. Surface roughness was measured with an atomic force microscope (Nano Scope IIIa, Multimode (Veeco, Santa Barbara, CA) in tapping mode. Standard tapping mode silicon cantilevers of "BS-Tap300" with a spring constant of 40 N/m and a resonance frequency of 300 kHz were used at ambient conditions. The radius of curvature of the atomic force microscope tips was nominally less than 10 nm. A scan rate of 0.3-1Hz was employed at a resolution of 512 pixels/line. Surface roughness measurement (R_{rms}), defined as the standard deviation of the elevation, was determined from 2 μm x 2 μm scans and is the average of at least four images scanned at different locations on the sample surface.

3 Results and Discussion

Superoleophobic surfaces, in particular, underwater superoleophobic surfaces, have aroused a particular interest for their resistance to oil fouling and great potential in many industrial and technological applications.[39-40] The key parameters for superamphiphobicity are still missing. For water repellency, topography is essential, along with the chemical identity of the surface itself.[6-9] Clearly, combining appropriate surface roughness with low-surface-energy materials is a prerequisite to amplify the surface's intrinsic wetting behaviour for the fabrication of superamphiphobic surfaces. To achieve a material with special underwater superoleophobicity and switchable superhydrophobicity–superhydrophilicity ZnO nanorods may represent as a good candidate. The strategy for the fabrication of multiscale surface features for superoleophobic coatings herein is schematically shown and detailed in the experimental section, (Fig. 1). The preparation of the superhydrophobic and underwater superoleophobic surfaces are based on surface

modification along with generation of surface micro-nano structures, which contributes to surface roughness and amplifies surface wetting behaviours.

A structure mimicking the lotus leaf was built by fabricating different arrays of PDMS microposts as modelling surfaces with base diameter d=10-25 μm, height h=1μm, centre-to-centre pitch=10-70 μm. Nanostructures were then introduced on the PDMS microstructured surface and further increase the surface roughness, by growing ZnO nanorods on the primary PDMS microposts using a simple low temperature hydrothermal method in aqueous solution for several hours.[41]

To increase the oleophobic property of the surface in air, tridecafluoro-1,1,2,2-tetrahydrooctyl)-1-trichlorosilane, TFTS) which has lower surface tension than that of oil, was deposited on the surfaces, and experiments with droplets on hydrophobic and both oleophilic and oleophobic surfaces in air were performed. It is known that fluorine is the most effective approach for lowering the surface free energy in view of the fact that the closest hexagonal packing of $-CF_3$ groups on the surface would give the lowest surface energy of the materials.[42] This approach provides an alternative means, rather than turning the geometric parameters through microfabrication, of controlling the surface wettability.

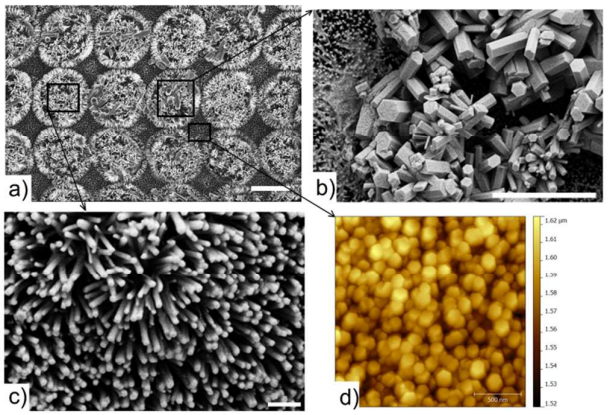

Fig. 2 Corresponding SEM images of the a) PDMS lotus leaf like hierarchical structure (scale bar 10 μm) and further magnifications of the ZnO nanorods (b)scale bar 5 μm,c) scale bar 500nm) d) AFM images of the ZnO nanorods.

Fig. 2 shows the typical SEM image of prickly PDMS-ZnO micro/nanostructures prepared after 6h hydrothermal treatment; it shows reveals the presence of a micro/nano-hierarchical structure at the front (adaxial), which mimic the dual tier roughness of the lotus leaf. All the micropillars and basal areas around the pillars were covered by densely aligned nanorods arrays. We should note that the ZnO nanorods on top of the pillars have a tendency to grow outward at the edge of the pattern, whereas the nanorods among the pillars grew vertically to the substrate. The slight difference of nanorods density may be due to the effects of the neighboring pillars, such that the surface coverage percentage among the pillars increased slightly being less spatially hindered and more edge confined.

Increase in length and diameter of ZnO nanorods grown on the microstructured PDMS surface were observed with the increased reaction time. A further magnification (Fig. 2c) suggests nearly vertically oriented arrays of ZnO nanorods (about 900 nm in length) densely covered the surface of microposts and flat surrounding areas with an average diameter of ≈ 90nm. The AFM image, (Fig. 2d), confirmed that the rods grow approximately perpendicular to the substrate surface and reveals the hexagonal structures of the ZnO nanorods. With the extension of reaction time, ZnO nanorods with larger dimensions were anchored to primary the ZnO nanorods, growing aslant with much larger lateral size and more intensive structure on the microstructures (Fig. 2b). The nanorods formed multi-pod structures, linked at a central point, which suggests a spontaneous nucleation in the solution is occurring. The reason for "dendrite-like" growth is that the nanostructured arrays may act as nucleation platforms for the preferential sites and rapid growth of larger nanorods and may show more available surface contact to the reaction solution. The fact that the nanorods grow at various angles with respect to the substrate could be attributed to the high misfit of the basal plane of the primary rods ZnO, resulting in non c-preferred oriented initial ZnO nuclei.

The motivation of the different size of the ZnO nanorods was related to be dependent on the ammonia amount present in solution. The key aspect of this process is the formation of $Zn(NH_3)_4^{2+}$ complexes. The supersaturation condition and reaction temperature results in affecting the interface-solvent interactions resulting in an increased concentration of Zn complexes in the solution which in turn enhances Zn supply for the formation of the ZnO rods.[43-44] A similar effect should then be responsible for the formation of the different growth size of the ZnO nanorods in our sample. After 6 h of reaction, a large number of longer nanorods grown from the centre of microposts and covered the surrounding areas on the substrate with diameters and lengths of about 100 nm and 2 μm. It indicated the higher surface area of microstructures exposed to zinc precursor solution increased the nuclei supersaturation and the ZnO nuclei on the micropillars could grow faster to form longer nanorods of ZnO than those on the flat areas.[45]

It is well known that the surface free-energy as well as the surface roughness influences the wettability of a surface. Liquids of different surface tensions were used to characterize the surface hydrophobicity and oleophobicity of the surfaces. The wetting behaviour in different phase systems (e.g. smooth PDMS surfaces, microstructured PDMS surfaces, micro/nano hierarchical structured surfaces and fluorinated micro/nano hierarchical structured surfaces) were investigated, (Fig. 3, Table 1). Fig. 3a, shows contact angles of oil (e.g., diiodomethane (γ_{lv} = 50.8 mN/m), and olive oil (γlv = 32.6 mN/m)) and water (γlv = 72.8 mN/m) on the the different solid surfaces for different systems. Flat PDMS showed a contact angle with water of about 116°, as indicated in Table 1.

Table 1 Contact angles in air of water, diiodomethane and oil droplets on different surfaces in different systems.

Liquids	Smooth PDMS	Micro-structured PDMS	Micro/nano-structured PDMS-ZnO surfaces	Micro/nano-structured fluorinated PDMS-ZnO surfaces
Water droplets (in air)	116.1±0.8°	120.8±2.5°	167.7±3.1°	137.3±1.9°
CH_2I_2 droplets (in air)	72.6±3.4°	86.8±1.7°	68.6±2.6°	101.3 ±1.8°
Oil droplets (in air)	43.2±2.8°	46.2±1.2°	9.1±1.5°	83.5±2.3°

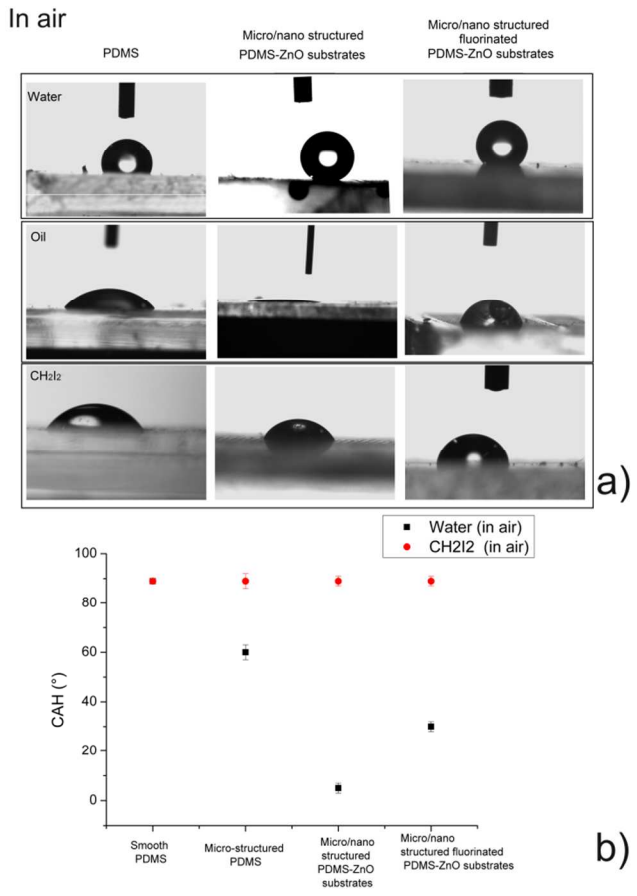

Fig. 3 Comparison of the wetting properties of the PDMS surface, micro/nano-structured PDMS- ZnO surfaces and fluorinated micro/nano-structured PDMS- ZnO surfaces, in air. a) Photographs of water, the oil and the diiodomethane droplets on the different surfaces in air. b) Contact Angle Hysteresis of the water and diiodomethane droplets on the different surfaces.

When the four surfaces were studied in an air system, it was found that all kinds of surfaces were hydrophobic or superhydrophobic. The CA of a water droplet on the micropatterned PDMS surface was slightly improved, as reported in Table 1, but the surface was still oleophilic in air. The contact angles of diiodomethane and olive oil of the smooth and micro-structured PDMS surface in air were much lower than 90°, as in fact PDMS is intrinsically oleophilic. The micro/nano-structured PDMS ZnO surface showed a dramatic increase of the hydrophobicity of the PDMS surface (water CA ~167.7± 3.1°) whereas it was still insufficient to realize superoleophobicity in air, showing instead an enhanced superoleophilicity, similarly to lotus leafs. To this end, oleophobic chemistry for the coating was achieved by fluoro-modifying the micro/nano-structured PDMS ZnO substrates with exposure to trichlorosilane, TFTS. After TFTS coating, the surfaces became oleophobic in air. The diiodomethane and olive oil CA was significantly increased to 101.37± 18° and 83.55 ± 2.3°, respectively (Fig. 3a). This result confirms that the fluorination of micro/nano-structured PDMS-ZnO surfaces presents a typical superhydrophobic property in air. However a decrease in the apparent water contact angle with a pinning behaviour to the surface was observed. This observation can be explained by considering that when a liquid comes in contact with a solid surface, it can either adopt the fully wetted Wenzel state or yield a composite liquid–air interface, known as the Cassie–Baxter state.[44-45] Typically, in the wetted Wenzel state, water is in complete contact with the rough solid, therefore by increasing surface roughness, the actual CA decreases for amphiphilic materials ($\theta<90°$) and increases for amphiphobic materials ($\theta>90°$). For a rough surface composed of solid and air, according to the theory developed by Cassie et al.,[46-47] stable air molecules exist on the surface of micro/nanostructures, forming a water/air/solid interface. When a rough surface comes into contact with water, air trapping in the pockets created by the rough area contributes greatly to the increase in hydrophobicity. The water droplet maintains the superhydrophobic Cassie–Baxter state on the hierarchical surfaces composed of two different scale of roughness (Fig. 3). Therefore the CA for water will increase and that for oil will decrease on the tier scale rough surface created by ZnO on the microposts, accordingly. Subsequent fluorination results in the contribution of TFTS deposits to the nanoroughness that counterbalances some possible smoothing effect of nanocomposite texture of the ZnO nanorods, annihilating the effect of the presence of the air pockets introduced by the prickly nature of the nanorods. Fig. 4 shows a SEM image of the morphology of the micro/nano structured fluorinated PDMS-ZnO substrate. Significant morphological changes are present. The morphological built up over the ZnO nanorods "smoothed over" the roughness which may explain the observed change of states of wettability of oil and water. The uniformity of the surface was also improved and therefore the decrease of the contact angle as well as the adoption of a fully wetting Wenzel mode. Besides the dynamic wetting behaviours are also very different. The contact angle hysteresis, (CAH) (quantified in terms of the difference between the advancing and receding contact angles) as well as the ability of a drop to slide off an inclined surface, are indicators of Wenzel to Cassie states.[48-50]

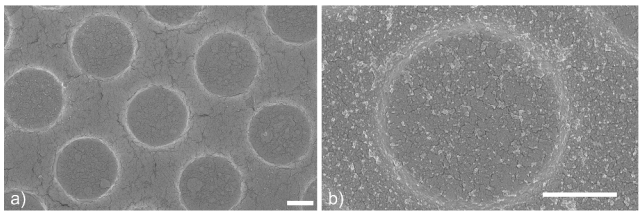

Fig. 4 Corresponding SEM images of the a) micro/nano structured fluorinated PDMS-ZnO surface showing that the complete coverage of the nanorods and consequent change of morphology; b) further magnification (scale bar 10 μm). The thickness of the coating was measured to be less than about 200 nm.

Surfaces with the Cassie state of wetting demonstrate small contact-angle hysteresis values and low sliding-angle values due to easy roll-off of the droplets; however, for the Wenzel state of wetting, droplets pin to the surfaces with high contact-angle hysteresis values. Unlike the contact angle, the sliding angle is strongly affected by the alignment and continuity of the three-phase contact line.[6-8,-51] The structural heterogeneity and chemical heterogeneity in the hydrophobic surface affect the sliding angles while pinning the three-phase contact lines.[46-48] The water sliding angles and contact-angle hysteresis of the micro/nano-structured PDMS-ZnO surfaces were very low in good accordance with the Cassie state (water CA_{adv} ~167.7± 2°, CA_{rec} ~162.2± 2°, and CAH ~ 5.5°). In fact, we observe a close to perfect rolling behaviour with modified roll-off angles of merely a few fractions of a degree. However, the PDMS microstructured surface and the fluorinated micro/nano-structured PDMS-ZnO surfaces, exhibit high contact angle hysteresis and large sliding angles Fig. 3b. A transition from the superhydrophobic Cassie to the superhydrophobic Wenzel state was therefore induced by exposure of the TFTS silane.

For underwater applications, the nature of oleophobicity/philicity of an oil droplet in water depends from the values of surface energies of various interfaces and contact angles of water and oil in air. In fact the surface tension of oil and organic liquids is lower than that of water, so to create a superoleophobic surface, the surface energy of the solid surface in air should be lower than that of oil. As reported in literature a key parameter for superoleophobic surface in water is it being superhydrophilic in air.[52-53] However, despite their low surface energies, the PDMS substrates are hydrophobic in air (Table 1). The underwater oil wettability of the different systems was evaluated by immersing the samples in aqueous media. Without treatments, the PDMS surface exhibited oleophilic property (i.e. diiodomethane 62.07±0.5° and oil 21.5±0.8°), Table 2, whereas the microstructured surface showed a negligible increase of the oil CA. However, the micro/nano-structured PDMS-ZnO surfaces, compared with the surface wettability to oil, showed improved underwater superoleophobicity with an oil contact angle (OCA) of 152.8 ±0.5° and 93.55±0.9°, of diiodomethane and oil respectively.

Table 2 Contact angles underwater of diiodomethane and oil droplets on different surfaces in different systems.

Surfaces systems	Smooth PDMS	Micro-structured PDMS	Micro/nano-structured PDMS-ZnO surfaces	Micro/nano-structured fluorinated PDMS-ZnO surfaces
CH_2I_2 droplets (in water)	62.1±1.9°	68.5±2.7°	152.8±1.2°	125.7±1.1°
Oil droplets (in water)	21.5±2.3°	25.7±3.1°	93.5±0.9°	91.2±2.1°

As a result, the measured advancing and receding contact angles of the diiodomethane droplet in water are 157.9 ± 1.2° and 150.2 ± 1.5°, respectively, the difference is so small that the diiodomethane droplet can easily roll off the micro/nano-structured PDMS- ZnO surface in water with a low sliding angle, (Fig. 5, Movie S1). The key point to discuss here is the mechanism of such under-water superoleophobic behaviour of the micro/nano-structured PDMS- ZnO. In this case, the rough nanostructure of the ZnO surface plays a key role in improving the oleophobicity under water triggering CB state, as depicted in Fig. 5.

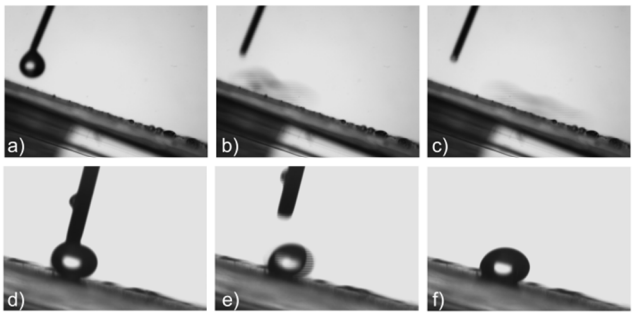

Fig. 5 Adhesive force of oil in water. a-c) A droplet of diiodomethane rolling off the micro/nano-structured ZnO surface as soon as the droplet made contact. d-f) Onto the fluorinated surface the drop firmly adhered to the surface and did not roll away indicating a Wenzel state. Roll off angle was ~10°.

In the solid-water-oil interface system, the oil droplet sits on water trapped in the micro and nano roughness. Furthermore, we found that these diiodomethane droplets were quite unstable on the PDMS-ZnO nanostructured surface and they could easily detach from the surface by gentle disturbance, suggesting a low adhesion of the surface to the oil droplets in the aqueous medium. This was explained considering that when the micro/nano structured PDMS-ZnO was immersed in water, the air is trapped in the rough nano posts formed by the ZnO on the surface posts and when diiodomethane droplet contacts such a surface, it forms a complex interfacial system, i.e., a four phase system (air–solid–oil–water).[54] The trapped air in the nano-structure greatly decreases the contact area between oil and solid surface, and forms the discontinuous triple phase contact line, largely improving the repellent force to oil. This state is equivalent to an underwater Cassie state of wetting.[55-56] The hierarchical type of structure contributes greatly to the

amphiphobicity increase and results in the super-antiwetting performance for water and diiodomethane.[57-58] To study optimization of oleophobicity in both solid-air water and solid-air-oil interfaces, the static contact angles for water and oil droplets were measured on the micro/nano-structured PDMS-ZnO surfaces with fluorosilane and are summarized in Table 2. After surface chemical coating with, the underwater CA of an oil droplet on the micropatterned PDMS was considerably reduced to ~ 125,7 ±2° in water. Moreover, this fluorinated surface suffered from high oil-adhesion, Movie S2. The oil sliding angle (SA) is found to be 52.6 ± 2.9°. Namely, the fluorinated sample although providing a low energy surface, revealed as well as a change of morphology of the rough 3D hierarchical nanostructure with limited roughness that induced this Wenzel state. Therefore, we believe that the underwater superoleophobic system relies on the combination of the micro and nanotextures of the ZnO nanorods.

Due to the ultralow adhesive force of oil in water, the micro/nano-structured PDMS-ZnO surface offers ideas to design surfaces for oil transportation with high efficiency and could be considered as a kind of self-cleaning anti-oil layer for practical applications. As shown in (Fig. 5 a-c, Movie S1), a droplet of oil, was dropped onto the surface, underwater. As soon as the oil droplet made contact with the micro/nano-structured ZnO surface it immediately rolled off. Once again, the micro/nano-structured PDMS-ZnO surface proved to be the most robust surface for the oil droplet to reside in the Cassie wetting regime. For comparison, we showed that the fluorinated surface did not exhibit the anti-oil ability. The oil droplet on the hierarchical microstructures firmly adhered to the surface and did not roll away indicating the water droplet was mostly in the Wenzel state, (Fig. 5 d-f, Movie S2). This also suggests that both the surface microstructures and surface chemistry were crucial to the self-cleaning anti-oil ability in underwater applications.

Previous reports have shown that bioinspired underwater oleophobic surfaces can be prepared based on two criteria: the first based on the hydrophilicity of the surface, (i.e. the presence of water molecules bonded to the surfaces would provide a repulsive force against oil immersion) and the second on asymmetric microtextures, (which drive the anisotropic motion of fluid on the surfaces).[5,19,41,59] In our approach, we show that a hydrophilic surface is not necessary to obtain underwater superoleophobicity, but an adequate micro/nano-structured texture is required that can trap air in or water in the pockets created by the rough area. Tuning the surface wettability is of great interest for both scientific research and practical applications. In order to evaluate the tuneable photoresponsiveness of surface wettability of water and oil, the micro/nano-structured and fluorinated micro/nano-structured PDMS-ZnO surfaces were placed under UV irradiation (Fig. 6). Analysis of the evolution of the wetting properties on ZnO nanorods surface upon increasing exposure of irradiation (Fig. 6c) demonstrates a decrease in air of the water CA down to ~54°. A similar decrease is seen with the diiodomethane both in air and in underwater systems. Simultaneously, oil droplets can be observed to spread out over the films at all irradiation stages in air, indicating constant superoleophilicity in air (oil CA ~9-11°) while in underwater systems a slight decrease was measured. However, due to the weak UV light intensity (40 $\mu W/cm^2$), CA can not reduce to 0° in a short time. If the UV irradiation time is increased to more than 80 h, a contact angle of less than 10° can be also acquired in this condition. As reported, gradual increase in hydrophilicity can be attributed to the formation of electron-hole pairs in the ZnO surface, and some of the holes can react with lattice oxygen to form surface oxygen vacancies on the surface of ZnO nanorods due to slow release of oxygen during UV illumination.[60] This phenomenon is considered to result from the dissociative competing of desorption of molecular oxygen from the zinc oxide surface followed by dissociative water adsorption generating photo-electrons and holes, which then react with oxygen and water to produce highly reactive species of superoxide anions and hydroxyl radicals. As a result, the surface hydrophilicity is improved. For a micro/nano structured surface, water will enter and fill the grooves of the nanorods, leaving only the up part of the microposts in contact with the liquid. This effect results in a non-complete spreading of the water CA. The effects of the chemical characteristics on the photoresponsive wettability of the surface the evolution of the contact angles of water and oils under UV irradiation were very strong. As shown (Fig. 6 c, d), the water contact angles of the fluorinated micro/nano-structured PDMS-ZnO remained almost unchanged after long-term UV irradiation, thereby displaying rather durable superhydrophobicity. Oil and diiodomethane were reduced slightly. Namely, this indicates that the chemical stability of fluorinated surface groups is not affected. We speculate that a possible reason for this behaviour may be related to the change of morphology as well as the chemical change of the substrate after fluoronisation. Subsequent prolonged storage of the substrates in the dark gradually re-establishes the initial hydrophobic character of the substrates. Again, the above evolution takes place with substantial preservation of the superoleophilicity and underwater superoleophobicity. The process of the reversible change of the CA can be carried out over several cycles of irradiation/dark storage (Fig. 6 e, f), both in air and underwater systems for the micro/nano structured substrates. As shown, a good reversibility was achieved between CA values after repeating for five cycles. Accordingly, these results indicated that the special interfacial properties of the chemical nature of the substrate and UV light illumination in both air and underwater systems have important effect on the photo-responsiveness wettability.

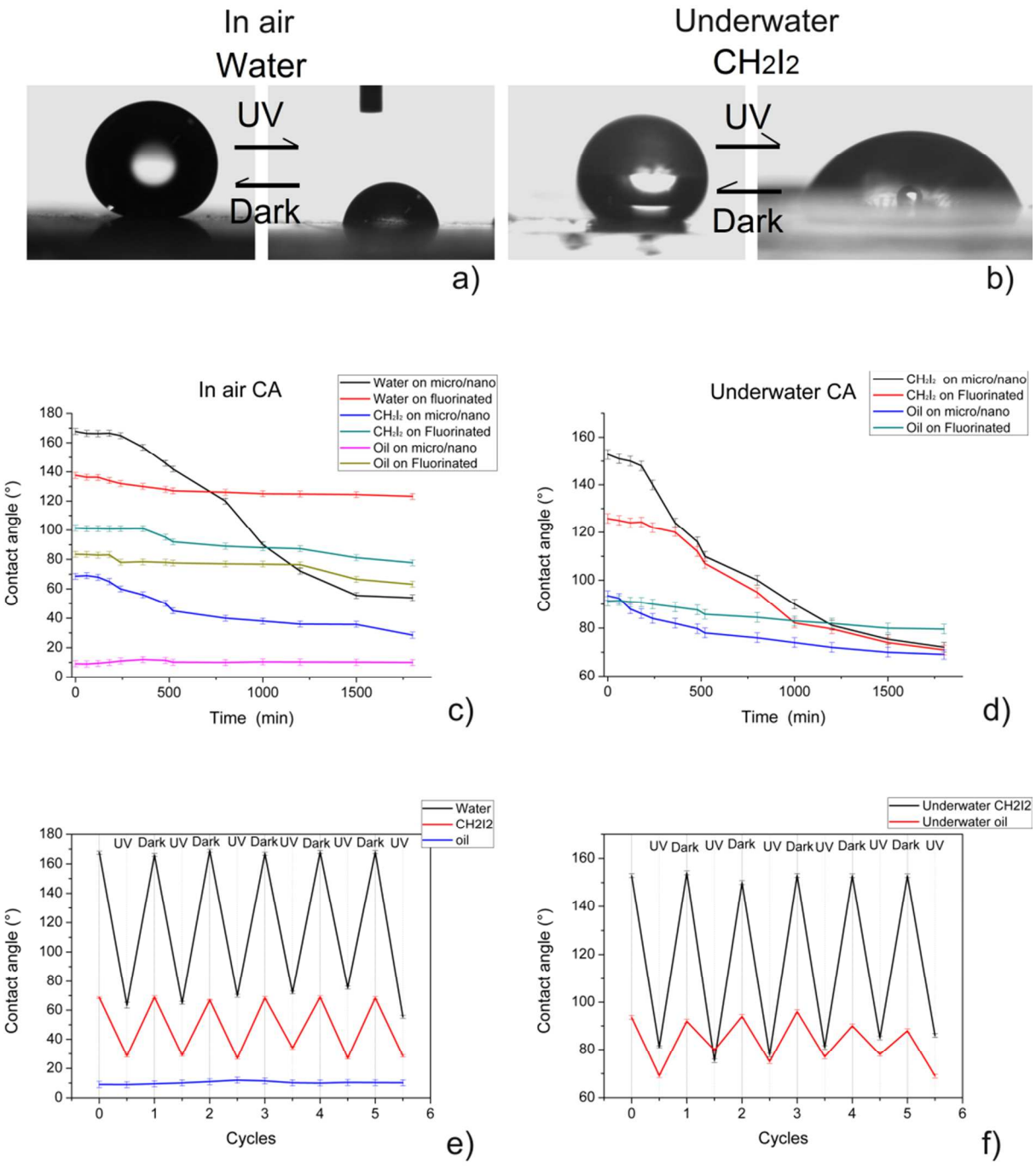

Fig. 6 Evolution of wettability and photo-switch repeatability on the micro/nano-structured PDMS-ZnO substrates. a-b) Photographs of water and the diiodomethane superhydrophobic droplets in air (a) and underwater (b) before and after UV irradiation. Water and oil contact angles of the micro/nano-structured PDMS-ZnO surfaces and fluorinated micro/nano-structured PDMS-ZnO surfaces under UV irradiation and after storage in the dark as a function of the UV irradiation, b) in air c) underwater. Reversible wettability of the water and oil CA on the micro/nano-structured PDMS-ZnO surfaces after storage in the dark and under UV irradiation e) in air f) underwater.

Durability of the micro/nano-structured PDMS- ZnO surfaces was evaluated by placing the samples in air and in water repeatedly several times. The wettability could be changed from being superhydrophobic in air to oleophobic under water (Fig. 7).

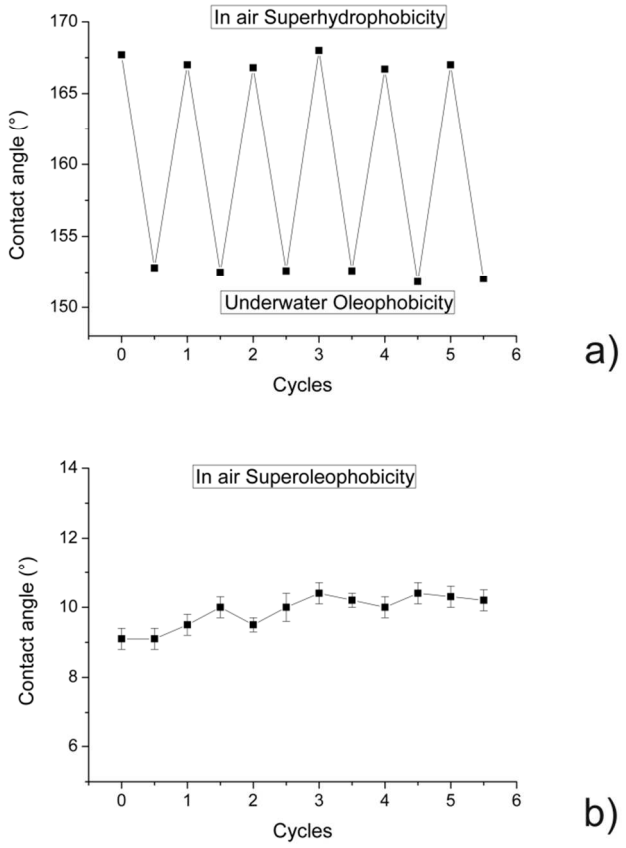

Fig. 7 The repeatable wettability of the micro/nano-structured PDMS-ZnO surfaces showing that a) the superhydrophobic behaviour in air and the underwater oleophobic property was stable after different cycles as well as the superoleophilic durability in air b), emphasizing the stability of the surfaces.

This process was repeated for several cycles. The repeatability remained even after three months without any special precaution. Moreover after immersion into water for different cycles it was found that the micro/nano-structured PDMS- ZnO surfaces were still superoleophilic, even after 24 h of immersion (Fig. 7), which demonstrates that the oleophilic property in air is relatively stable under water. We also evaluated the time dependence of the wettability in terms of the contact angles of water; droplets positioned on the fluorinated micro/nano-structured PDMS-ZnO possessed near-spherical shapes for over 30 min (the water droplet could still be moved readily at that time), suggesting stable superhydrophobicity. Because the fluorinated micro/nano-structured PDMS-ZnO possessed UV-durable superhydrophobicity, these surfaces might have potential applications in outdoor uses. Such coating can be applied to many surfaces to realize tunable wettability for biological, chemical and electrical applications.

Finally, robustness of the surface coating was tested with a standardized scotch tape test (ASTM).[61] The ZnO microstructured substrate showed an average water CA and CA hysteresis of 161.1° and 16.4°, respectively, which indicates that the superhydrophobicity was retained. Also underwater superoleophobic behaviour was still observed. The slight decrease of CA and increase of CA hysteresis, are likely due to contamination of the surface from the scotch, although partial destruction of the nanometer-scale structures cannot be excluded. In addition superhydrophobicity was maintained even after repeating bending of the substrate. These results indicate that adhesive force between ZnO nanorods and PDMS is relatively high.

Conclusions

Superhydrophobic/superoleophobic and self-cleaning surfaces are desirable for many industrial applications. Oleophobic surfaces have the potential for self-cleaning and antifouling from biological and organic contaminants in both air and underwater applications. An approach to realize a biomimetic superhydrophobic in air, oleophobic in water PDMS-ZnO surface were successfully developed using a typical and environmentally friendly solution-based hydrothermal method to form ZnO nanostructures. The developed structures exhibited water CA of above 160° and SA of less than 5° and superoleophilic behaviour in air, which made them well comparable to the natural lotus leaf. The higher water CA and lower SA were supposedly attributed to their unique dual-size (micro- and nano-scale) roughness leading to the minimization of surface energy. Furthermore, the micro/nano-structured PDMS-ZnO surfaces were found to be superbly oleophobic underwater. Generally a surface chemistry that is both oleophilic and hydrophobic is required to realize oleophilicity in aqueous media. In our case we obtained an underwater superoleophobicity which can effectively prevent the PDMS-ZnO surface from being polluted by oils. While the as-prepared micro/nano-structured PDMS-ZnO surfaces are superoleophilic, chemical functionalization with low surface energy molecules, such trichlorosilane TFTS, led the formation of oleophobic substrates in air. On the other hand underwater, the chemical functionalization reduced the superoleophobic behaviour of the diiodomethane, by influencing surface morphology. Again the micro/nanoscale hierarchical structure of the PDMS-ZnO surface played a dominant role in controlling the oil-adhesion behaviour of underwater superoleophobic, showing lower oil adhesion than fluorinated samples. Only few examples of surfaces on which oils form almost spherical droplets have been reported before.[16, 29] To the best of our knowledge, this is one of the first flexible surfaces that display underwater superoleophobicity with ultra-low contact angle hysteresis with low-surface-tension liquids, such as oil. The results provide new insights into how to control the wettability on PDMS-ZnO surfaces by adjusting the topographical structure and surface chemistry. For an oleophobic surface, oil contaminants are washed away when immersed in water. This work is promising in photo-induced water–oil mixture treatments such as oil/water separation and may also provide interesting insights into the design of novel functional devices based on controllable surface wettability. This effect leads to self-cleaning that can be used against ship fouling.

Acknowledgements

This work was supported by EFOR-CNR, PON-MAAT (Project number: PON02_00563_3316357), and funded by the Regione Puglia (APQ-Reti di Laboratorio, Project PHOEBUS, cod. 31). The authors are also grateful to Cristina Riccucci for useful technical support.

Notes and references

[a]National Nanotechnology Laboratory-Institute Nanoscience-CNR (NNL-CNR NANO), via Arnesano, 73100 Lecce, Italy
[b]Department of Physics, University Sapienza, P. le A. Moro 2, 00185, Rome, Italy
E-mail: barbara.cortese@nano.cnr.it
[c]Center for Life Nano Science@Sapienza, Istituto Italiano di Tecnologia,Viale Regina Elena 291, 00161,Roma, ITALY
[d]Department of Mathematics and Physics, University of Salento, Lecce, Italy
[e]Center for Biomolecular Nanotechnologies (CNB) of Italian Institute of Technology (IIT), Lecce, Italy;

Electronic Supplementary Information (ESI) available: Movie S1 showing the underwater oil slipping off a micro/nano-structured PDMS-ZnO surface, and Movie S2 showing the underwater oil adhesion on a fluorinated micro/nano hierarchical structured surface. See DOI: 10.1039/b000000x/

1 Y. Zheng, X. Gao and L. Jiang, *Soft Matter,* 2007, **3**, 178.
2 Y. Liu, X. Chen and J. H. Xin, *Bioinspiration and Biomimetics,* 2008, **3**, 046007.
3 X. Gao and L. Jiang, *Nature,* 2004, **432**, 36.
4 L. Zhai, M. C. Berg, F. Ç. Cebeci,Y. Kim, J. M. Milwid, M. F. Rubner and R. E. Cohen, *Nano Letters,* 2006, **6**, 1213.
5 M. Liu, S. Wang, Z. Wei, Y. Song and L. Jiang, *Adv. Mater*., 2009, **21**, 665-669.
6 B. Cortese, S. D'Amone, M. Manca, I. Viola, R. Cingolani and G. Gigli, *Langmuir*, 2008, **24**, 2712.
7 L. Feng, Z. Zhang, Z. Mai, Y. Ma, B. Liu, L. Jiang and D. Zhu, *Angew. Chem. Int. Ed*., 2004, **43**, 2012
8 B. Cortese, D. Caschera, F. Federici, G. M. Ingo and G. Gigli, *J. Mater. Chem. A*., 2014, **2**, 6781.
9 A. Tuteja, W. Choi, M. Ma, J. M. Mabry, S. A. Mazzella, G. C. Rutledge, G. H. McKinley and R. E. Cohen, *Science*, 2007, **318**, 1618.
10 B. Cortese and H. Morgan, *Langmuir*, 2012, **28**, 896.
11 L. Feng, S. Li, Y. Li, H. Li, L.Zhang, J. Zhai, Y. Song, B. Liu, L. Jiang and D. Zhu, *Adv. Mater.*, 2002, **14**, 1857.
12 X. M. Li, D. Reinhoudt and M. Crego-Calama, *Chem. Soc. Rev*., 2007, **36**, 1350.
13 Y. Y. Yan, N. Gao and W. Barthlott, *Adv. Colloid Interface Sci*., 2011, **169**, 80.
14 K. Tsujii, T. Yamamoto, O. Tomohiro and S. Shibuichi, *Angew. Chem. Int. Ed*., 1997, **36**, 1011.
15 M. Liu, S. Wang, Z. Wei, Y. Song and L. Jiang, *Adv. Mater.,* 2009, **21**, 665.
16 H. Wang, Y. Xue, J. Ding , L. Feng, X. Wang and T. Lin , *Angew. Chem. Int. Ed*., 2011, **50**, 11433.
17 H. Jin, M. Kettunen, A. Laiho, H. Pynnönen, J. Paltakari, A. Marmur, O. Ikkala and R. H. A. Ras, *Langmuir,* 2011, **27**, 1930.
18 L. Cao, T. P. Price, M. Weiss and D. Gao, *Langmuir,* 2008, **24**, 1640.
19 Y. Cai, L. Lin, Z. Xue, M. Liu, S. Wang and L. Jiang, *Adv. Funct. Mater*., 2014, **24**, 809.
20 Y. C. Jung, B. Bhushan, *Langmuir,* 2009, **25**, 14165.
21 L. Lin, M. Liu, L. Chen, P. Chen, J. Ma, D. Han and L. Jiang. *Adv. Mater*., 2010, **22**, 4826.
22 L. Vayssieres, *Adv. Mater*. 2003, **15**, 464.
23 A. K. Kota, J. M. Mabry and A. Tuteja, *Surface Innovations*, 2013, **1**, 71.
24 S. Shibuichi, T. Yamamoto, T. Onda and K. Tsujii, *J. Colloid Interface Sci*., 1998, **208**, 287.
25 H. Li, X. Wang, Y. Song, Y. Liu, Q. Li, L. Jiang and D. Zhu, *Angew.Chem., Int. Ed*., 2001, **40**, 1743.
26 M. Kiuru and E. Alakoski, *Mater. Lett*., 2004, **58**, 2213.
27 Q. Xie, J. Xu, L. Feng, L. Jiang, W. Tang, X. Luo and C. C. Han, *Adv.Mater*., 2004, **16**, 302.
28 M. Nicolas, F. Guittard and S. Geribaldi, *Angew. Chem., Int. Ed*., 2006, **45**, 2251.
29 H. F. Hoefnagels, D. Wu, G. de With and W. Ming, *Langmuir,* 2007, **23**,13158.
30 A. Tuteja, W. Choi, J. M. Mabry, G. H. McKinley and R. E. Cohen, *Proc. Natl. Acad. Sci. USA,* 2008, **105**, 18200.
31 W. Choi, A. Tuteja, S. Chhatre, J. M. Mabry, R. E. Cohen and G. H. McKinley, *Adv. Mater,*. 2009, **21**, 2190.
32 W. C. Wu, X. L. Wang, D. A. Wang, M. Chen, F. Zhou, W. M. Liu and Q. J. Xue, *Chem. Commun*., 2009, 1043
33 A. K. Kota, G. Kwon, W. Choi, J. M. Mabry and A. Tuteja, *Nature Communications,* 2012, **3**,1025.
34 L. Zhang, Z. Zhang and P. Wang, *NPG Asia Materials,* 2012, **4**, e8.
35 A. Nakajima, K. Hashimoto, T. Watanabe, K. Takai, G. Yamauchi and A. Fujishima, *Langmuir,* 2000, **16**, 7044.
36 D. Tian, Z. Guo, Y. Wang, W. Li, X. Zhang, J. Zhai and L. Jiang, *Adv. Funct. Mater*., 2014, **24**, 536.
37 C. F. Wang, F. S. Tzeng, H. G. Chen and C. J. Chang, *Langmuir* 2012, **28**, 10015.
38 D. Tian, X. Zhang, Y. Tian, Y. Wu, X. Wang, J. Zhai and L. Jiang, *J. Mater. Chem*., 2012, **22**, 19652.
39 X. Deng, L. Mammen, H.J. Butt and D Vollmer, *Science*, 2012, **335**, 67 .
40 Z. Chua and S. Seeger, *Chem. Soc. Rev*., 2014, **43**, 2784.
41 J. Jiang, F. Gu, W. Shao, L. Gai, C. Li and G. Huang, *CrystEngComm,* 2011, **13**, 4861.
42 E. F. Hare, E. G. Shafrin and W. A. Zisman, *J. Phys. Chem*.,1954, **58**, 236.
43 L. L. Yang, Q. X. Zhao, M. Willander, X. J. Liu, M. Fahlman and J. H. Yang, *Cryst. Growth Des,*. 2010, **10**, 1904.
44 P. Tonto, O. Mekasuwandumrong, S. Phatanasri, V.Pavarajarn and P. Praserthdam, *Ceramics International*., 2008, **34**, 57.
45 N. Boukos, C. Chandrinou, K. Giannakopoulos, G. Pistolis and A. Travlos *Appl. Phys. A.,* 2007, **88**, 35.
46 D. Quere, *Annu. Rev. Mater. Res*., 2008, **38**, 71

47 M. S. Bobji, S. V. Kumar, A. Asthana and R. N. Govardhan, *Langmuir*, 2009, **25**, 12120.
48 M. Callies and D. Queré, *Soft Matter,* 2005, **1**, 55.
49 N. A. Patankar, *Langmuir*,2004, **26**, 7498.
50 L. Gao and T. J. McCarthy, *Langmuir,* 2007, **23**, 3762.
51 W. Wu, Q. Zhu, F. Qing and C. C. Han, *Langmuir,* 2009, **25**, 17.
52 M. J. Liu, S. Wang, Z. Wei, Y. Song and L. Jiang, *Adv. Mater*., 2009, **21**, 665.
53 D. Wu, S. Z. Wu, Q. D. Chen, S. Zhao, H. Zhang, J. Jiao, J. A. Piersol, J. N. Wang, H. B. Sun and L. Jiang. *Lab Chip*., 2011, **11**, 3873.
54 M. Jin, J. Wang, X. Yao, M. Liao, Y. Zhao and L. Jiang. *Adv. Mater.*, 2011, **23**, 2861.
55 A. Marmur, *Langmuir,* 2006, **22**, 1400.
56 R. Poetes, K. Holtzmann, K. Franze and U. Steiner, *Phys. Rev. Lett*., 2010, **105**, 166104.
57 Y. K. Lai, X. Ga, H. Zhuang, J. Huang, C. Lin and L. Jiang, *Adv. Mater*. 2009, **21**, 3799.
58 Z. X. Xue, S. Wang, L. Lin, L. Chen, M. Liu, L. Feng and L. Jiang, *Adv. Mater*., 2011, **23**, 4270.
59 X. Feng, L. Feng, M. Jin, J. Zhai, L. Jiang and D. Zhu, *J. Am. Chem. Soc*., 2004, **126**, 62.
60 R. D. Sun, A. Nakajima, A. Fujishima, T. Watanabe and K. Hashimoto, *J. Phys. Chem.B*., 2001,**105**, 1984.
61 ASTM Ann. Book ASTM Standards.

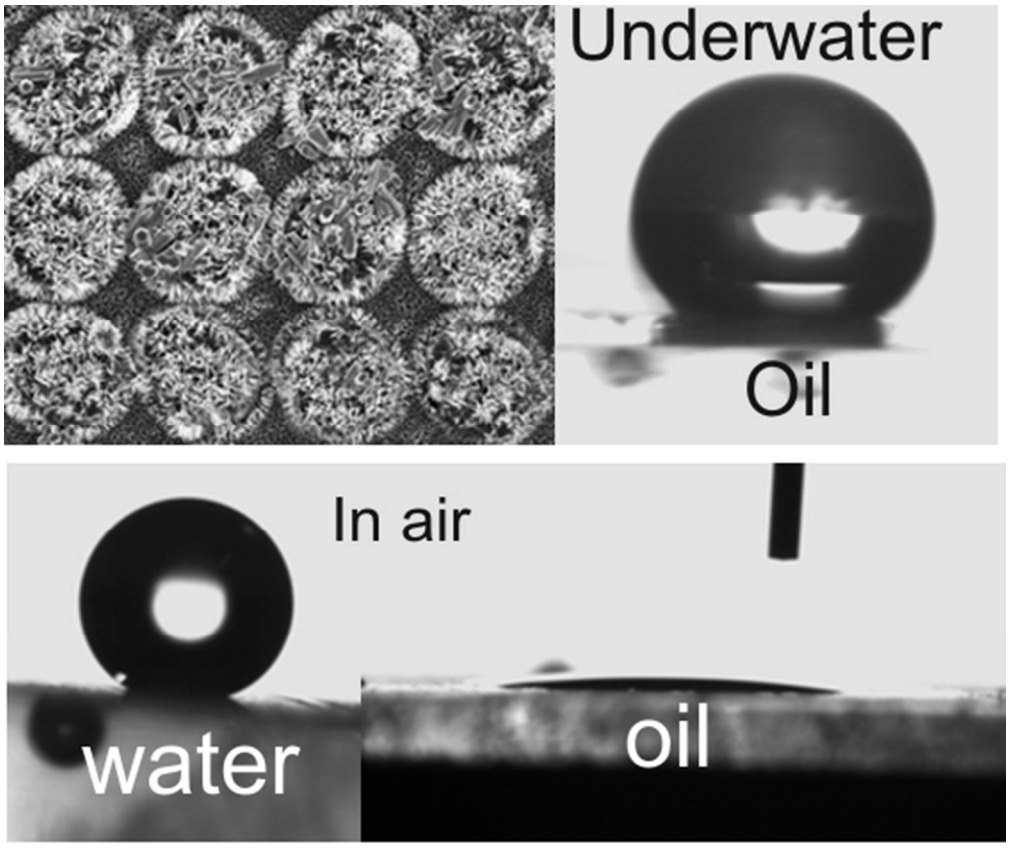

Surfaces with underwater superoleophobic efficacy and superhydrophobic/oleophilic property in air were created with ZnO nanostructures on PDMS microstructures.
47x39mm (300 x 300 DPI)